Ocean Engineering

Manoeuvring prediction of pusher barge in deep and shallow water

A. Maimun, A. Priyanto, **A.H. Muhammad**, C.C. Scully, Z.I. Awal

Pages 1291-1299 Volume 38, Issues 11–12, Pages 1277-1356 (August 2011)

Ocean Engineering

An International Journal

USA mailing notice: *Ocean Engineering* (ISSN 0029-8018) is published monthly, January to December by Elsevier Ltd., The Boulevard, Langford Lane, Kidlington, Oxford OX5 1GB, UK. Periodical postage paid at Rahway NJ and additional mailing offices.
USA POSTMASTER: Send change of address to *Ocean Engineering*, Elsevier Customer Service Department, 3251 Riverport Lane, Maryland Heights, MO 63043, USA.
AIRFREIGHT AND MAILING in USA by Mercury International Limited, 365, Blair Road, Avenel, NJ 07001.

Elsevier Ltd.
The Boulevard, Langford Lane, Kidlington, Oxford OX5 1GB, U.K.
Elsevier Inc.
655 Avenue of the Americas, New York, NY 10010, U.S.A.

Ocean Engineering 38 (2011) 1291–1299

Contents lists available at ScienceDirect

Ocean Engineering

journal homepage: www.elsevier.com/locate/oceaneng

Manoeuvring prediction of pusher barge in deep and shallow water

A. Maimun*, A. Priyanto, A.H. Muhammad, C.C. Scully, Z.I. Awal

Department of Marine Technology, Faculty of Mechanical Engineering, Universiti Teknologi Malaysia, Skudai 81310, Malaysia

ARTICLE INFO

Article history:
Received 16 November 2009
Received in revised form
27 October 2010
Accepted 15 May 2011
Editor-in-Chief: A.I. Incecik
Available online 25 June 2011

Keywords:
Pusher barge
Turning circle
Zig-Zag manoeuvring
Shallow water
Deep water

ABSTRACT

This paper presents an experimental investigation on the manoeuvring characteristics of a pusher-barge system for deep ($H/d > 3$) and shallow water ($H/d = 1.3$) condition. Since, the operation of pusher-barge mainly concentrates on confined waters, there is a need to predict and analyze the manoeuvring characteristic of the system for a safe and acceptable performance. A time domain simulation programme was developed for this purpose. A series of model experiments were carried out to determine the hydrodynamic coefficients using a planar motion mechanism (PMM). The time domain simulation shows the manoeuvring characteristic in the form of turning circle trajectories and zig-zag manoeuvre based on the hydrodynamic coefficients, which were derived based on experimental results. The manoeuvring characteristics in shallow and deep water conditions were compared through the simulation results. A comparison of simulation results based on experimental and empirical driven coefficients for both conditions shows that the experimental coefficients gave better manoeuvring characteristics for both turning circle trajectories and zig-zag manoeuvre.

1. Introduction

Presently, the most economical means of carrying goods in inland waterways for Indonesia and Malaysia is through barges. However, the use of barges in towing mode could affect its safety, as it has to manoeuvre in rivers of confined waters. In order to enhance safety there is growing use of pusher-barge systems for carriage of cargoes, which is an alternative mode of transportation in inland waterways and coastal regions that offered a minimum operating cost and safety. This system must have good manoeuvring capabilities to maintain its intended course in inland waterways, coastal area and in ports. The pusher barge must also be able to stop within a reasonable distance or turn within the reasonable turning path in order to avoid some hazardous conditions, such as collision, ramming and grounding.

Manoeuvring characteristic of a pusher barge is dependent on the parameters of the waterways such as bank shape and water depth (Lataire et al., 2007). Vantorre and Eloot (1996) compared different formulations of lateral force and yawing moment with model experiment results for shallow water manoeuvring for all drift angles and found that a tubular formulation of the lateral force and the yawing moment was needed to cover the whole range of drift angles. According to Beukelman and Journee (2001), deduction of water depth causes an increase of moment and lateral force, which will reduce the manoeuvring capability of a vessel.

Since steering and manoeuvring describes the pusher barge motions on a horizontal plane, atime domain coupled equation may be developed to describe the motions. The coefficients of the various terms in the equation are referred to as the hydrodynamic derivatives. These derivatives are dependent upon the hydrodynamic flow around the ship hull, which in turn depends on the geometry of the submerged body of the hull (Wang et al., 2000). This research focuses on a simulation programme, which was developed based on the hydrodynamic coefficients to predict the manoeuvrability of the pusher barge.

2. Mathematical model

The mathematical model for manoeuvring motion can be described by the following equation of motion, using the coordinate system in Fig. 1.

$$X = \tfrac{1}{2}\rho L^2 d(m' + m'_x)\dot{u} - \tfrac{1}{2}\rho L^2 d(m' + m'_y) r v$$

$$Y = \tfrac{1}{2}\rho L^2 d(m' + m'_y)\dot{v} + \tfrac{1}{2}\rho L^2 d(m' + m'_x) r u \quad (1)$$

$$N = \tfrac{1}{2}\rho L^4 d(I'_{zz} + J'_{zz})\dot{r}$$

where m, m_x, and m_y are the mass of ship, and added mass in x- and y-directions, respectively; I_{ZZ} and J_{zz} moment of inertia and add moment of inertia around z-axis, respectively; β is Drift angle at the centre of gravity C.G. [$\beta = -\sin^{-1}(v/U)$]; r' is dimensionless turning rate [$r' = r(L/U)$]; r and v are the turning rate and sway

*Corresponding author. Tel.: +60 75534744; fax: +60 75566159.
E-mail address: adi@fkm.utm.my (A. Maimun).

0029-8018/$ - see front matter © 2011 Elsevier Ltd. All rights reserved.
doi:10.1016/j.oceaneng.2011.05.011

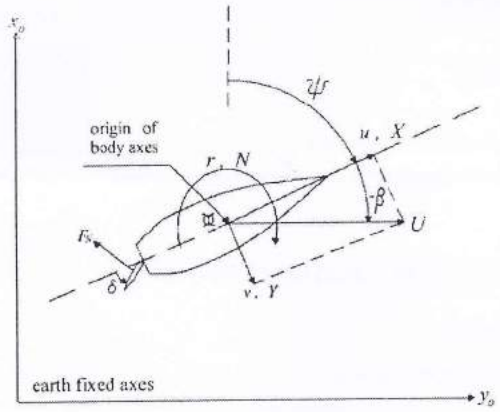

Fig. 1. Co-ordinate system.

velocity, respectively; and L, d and u are the ship length, ship draught and ship speed, respectively

The superscript {′} in the equations refers to the non-dimensional quantities defined by:

$$m',m'_x,m'_y=\frac{m,m_x,m_y}{0.5\rho L^2 d};\quad I'_{zz}J'_{zz}=\frac{I_{zz}J_{zz}}{0.5\rho L^4 d}$$

As shown in Fig. 1, (U) is the actual ship velocity that can be decomposed in an advance velocity (u) and a transversal velocity (v). The Pusher-Barge has also a rotation velocity with respect to the z-axis. This axis is normal to the XY plane and passes through the Pusher-Barge centre of gravity (C.G). (β) is the angle between U and the x-axis and it is called drift angle. (Ψ) is the Pusher-Barge heading angle and (δ) is the rudder angle. X,Y and N represents the hydrodynamic force and moment acting on the mid ship of hull. These forces can be described separating into the following component from the viewpoint of the physical meaning.

$$X=X_H+X_R+X_P \tag{2}$$

$$Y=Y_H+Y_R+Y_P \tag{3}$$

$$N=N_H+N_R+N_P \tag{4}$$

where, the subscripts H, P and R refer to hull, propeller and rudder, respectively, according to the concept of MMG expression.

2.1. Forces and moment acting on Hull

X_H, Y_H and N_H are approximated by the following polynomials of β and r'. The coefficients of polynomials are called hydrodynamic coefficients.

$$X_H=\tfrac{1}{2}\rho LdU^2(X'_{\beta r}r'\sin\beta+X'_{uu}\cos^2\beta)$$

$$\begin{aligned}Y_H=&\tfrac{1}{2}\rho LdU^2(Y'_\beta\beta+Y'_r r'+Y'_{\beta\beta}\beta|\beta|+Y'_{rr}r'|r'|+Y'_{\beta\beta\beta}\beta^3\\&+Y'_{rrr}r'^3+(Y'_{\beta\beta r}\beta+Y'_{\beta rr}r')\beta r')\end{aligned} \tag{5}$$

$$\begin{aligned}N_H=&\tfrac{1}{2}\rho L^2dU^2(N'_\beta\beta+N'_r r'+N'_{\beta\beta}\beta|\beta|+N'_{rr}r'|r'|\\&+N'_{\beta\beta\beta}\beta^3+N'_{rrr}r'^3+(N'_{\beta\beta r}\beta+N'_{\beta rr}r')\beta r')\end{aligned}$$

The calculation method of forces and moment induced by propeller can be referred in Appendix A.

2.2. Determination of hydrodynamic coefficient

Success of the manoeuvring prediction depends heavily on the knowledge of the hydrodynamic coefficients and the ways to estimate them. This research involves model testing and empirical methods to determine the hydrodynamics coefficients for the simulation. Hydrodynamic coefficients based on model testing method are obtained by the measurement of forces from planar motion mechanism (PMM). The empirical method is based on an approximation formulas to determine the hydrodynamic coefficients. In this case, the Kijima's formula will be used as a reference. This formula is obtained semi-empirically from the results of numerical calculations based on lifting surface theory and model tests in full load condition. The shallow water coefficients are obtained by multiplying a correction factor with coefficients in deep water condition (Maimun et al., 2005).

$$D_{shw}=f(h)D_{dep}$$

where D_{shw} is the derivatives in shallow water including ballast and half load conditions, D_{dep} is derivatives in deep water including ballast and half load conditions and $f(h)$ is correcting factor

Kijima's approximation formula is further explained in Appendices B and C.

3. Experiment

The experiment was conducted in the 120 m long towing tank at Marine Technology Laboratory of Universiti Teknologi Malaysia (UTM). Captive model tests are carried out using a planar motion mechanism (PMM) to determine the hydrodynamic coefficients of the pusher barge.

The model was connected to the PMM by means of one longitudinal and two transverse force transducers fitted in ball-jointed rods, allowing heave, pitch and roll. The transducer in longitudinal direction is more sensitive than the transducers as applied in transverse direction in order to increase the accuracy of the measurements.

3.1. Data collection

In the experiment, the hydrodynamic forces and moments are measured in both deep water and shallow water. The deep water condition has a water depth to vessel draught ratio H/d greater than 3 and in shallow water H/d of 1.3. The principal particulars of these ship models are listed in Table 1.

Oscillatory model tests results are used to develop the hydrodynamic coefficients as input in mathematical modelling. Measurements of hydrodynamic forces and moments are shown with ship model from Figs. 2–9 as an example. The model will experience oscillatory motion while being towed in the tank at constant speed. The motion generated by PMM could be drift tests, pure sway, pure yaw, and yaw with drift test. The model is also free to heave and pitch, but restrained in surge, sway, and yaw motions. The input parameters of these tests are presented in Table 2.

Hull force and moment coefficients: X_H, Y_H and N_H are determined based on measurement by force transducers on the PMM.

Table 1
Principal dimensions of pusher and barge.

	Pusher		Barge		Pusher-barge	
	Full scale	Model	Full scale	Model	Full scale	Model
Lal (m)	29.76	0.5952	95	1.9	117.92	2.358
Lpp (m)	25	0.5	94.5	1.89	116.71	2.3342
B (m)	10.208	0.2042	19	0.38	19	0.38
d (m)	3.7	0.0740	4.75	0.095	4.75	0.095
Volume (m^3)	542.147	0.004446	7502.5	0.0615	7805.74	0.06401
CB	0.5746	0.5746	0.8797	0.8797	0.723	0.723

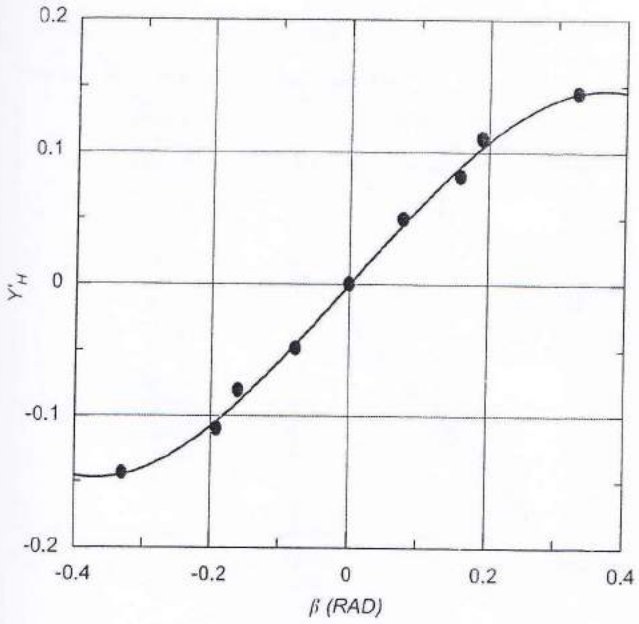

Fig. 2. Sway force (pure sway-deep water).

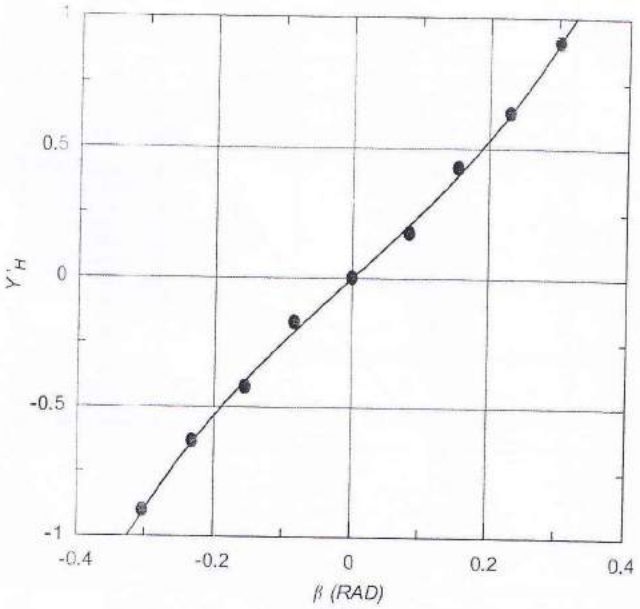

Fig. 4. Sway force (pure sway-shallow water).

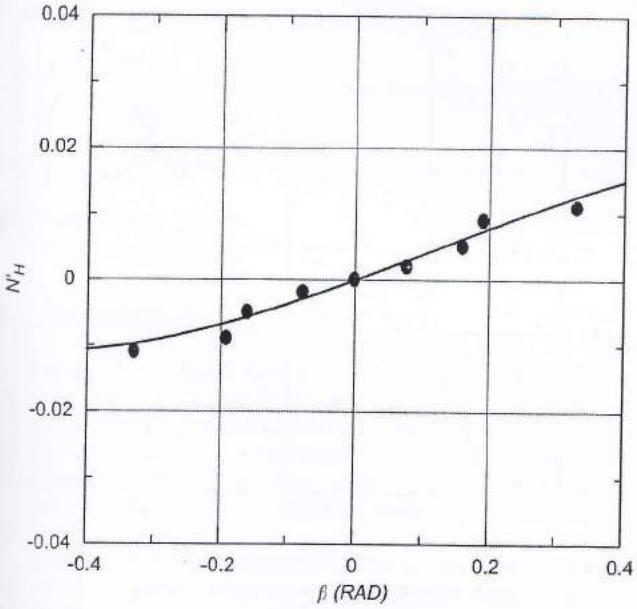

Fig. 3. Yaw moment (pure sway-deep water).

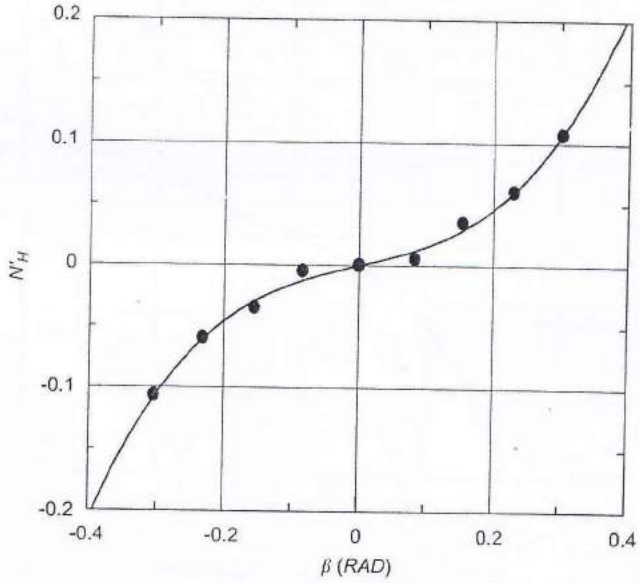

Fig. 5. Yaw moment (pure sway- shallow water).

Forces and moments are made non-dimensional by $\rho LdU^2/2$ and $\rho L^2dU^2/2$, respectively, and plotted against drift angle, as shown in Figs. 6–9. Coefficients based on experimental and empirical methods are compared in Table 3. Comparison of manoeuvrability of the pusher barge will take place once these coefficients are imported as parameters in the simulation.

4. Time domain simulation

The components of forces in the equation of motion were calculated corresponding to the prescribed manoeuvring motions. The vessel's swept path can based on the input of hydrodynamic coefficients in the simulation. The swept path is by double integrating the acceleration of the vessel in surge, sway and yaw axis of the mathematical model. In this case, Matlab Simulink programs were used to create numerical simulation of the turning and zig-zag manoeuvres (Kijima et al., 2000).

The equations of motion in this time domain simulation are then solved by numerical integration Dormand–Prince Method (Maimun et al., 2005). This method is included in one of the Mathlab ODE suites. The Mathlab ODE suites is a collection of five user-friendly finite-difference codes for solving initial value problems given by first-order systems of ordinary differential equations and their numerical solutions. The three codes (ode23), (ode45), and (odell3) are designed to solve non-stiff problems and the two codes (ode23s) and (odel5s) are designed to solve both stiff and non-stiff problems. (Ode45) was used in the simulation programme with variable time steps integration to avoid errors in some critical condition.

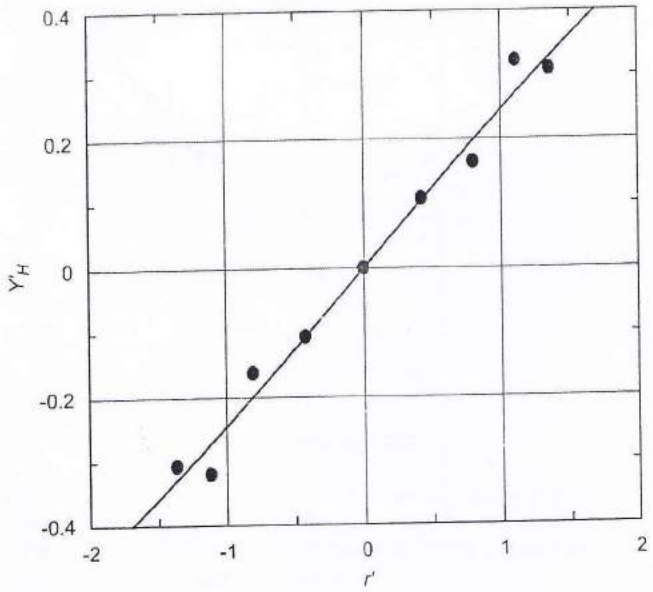

Fig. 6. Sway force (pure yaw-deep water).

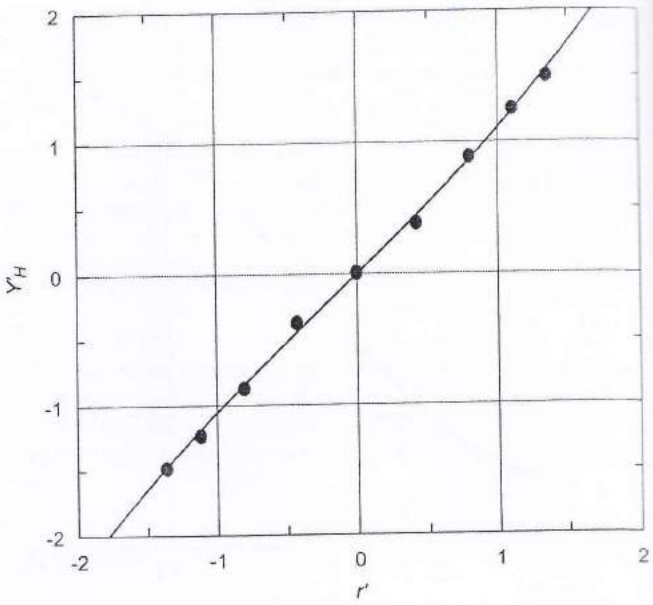

Fig. 8. Sway force (pure yaw-shallow water).

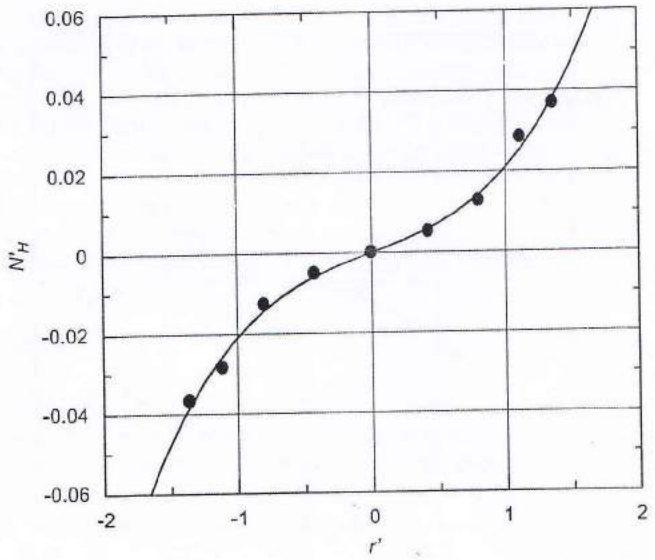

Fig. 7. Yaw moment (pure yaw-deep water).

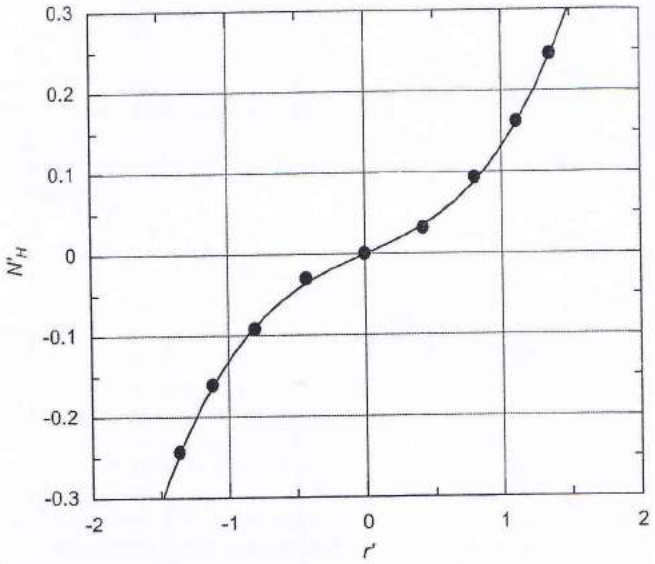

Fig. 9. Yaw moment (pure yaw-shallow water).

4.1. Simulation equation

The equations in the system of a three degree of freedom motions is used in the simulation and is based on the concept of the modular manoeuvring model. Whereby each element consisting of hull, propellers, and rudders- is represented by a self-contained and discrete module. The surge, sway, and yaw force equations are presented as follows:

$$X = \tfrac{1}{2}\rho L^2 d(m' + m'_x)\dot{u} - \tfrac{1}{2}\rho L^2 d(m' + m'_y)rv$$

$$Y = \tfrac{1}{2}\rho L^2 d(m' + m'_y)\dot{v} + \tfrac{1}{2}\rho L^2 d(m' + m'_x)ru \quad (6)$$

$$N = \tfrac{1}{2}\rho L^4 d(I'_{zz} + J'_{zz})\dot{r}$$

The equations can be rewritten in an acceleration form:

$$\dot{u} = (X + \tfrac{1}{2}\rho L^2 d(m' + m'_y)rv)/(\tfrac{1}{2}\rho L^2 d(m' + m'_x))$$

Table 2
Input parameters of PMM test.

Model test	Drift angle (deg.)	Oscillator amp (m)	Phase angle of oscillator arm (deg)
Drift test	0°, 4°, 8°, 12°, 16°	0	0
Pure sway	0°	0.1–0.4	0
Pure yaw	0°	0.1–0.4	33.02°
Yaw with drift	4°, 8°, 12°, 16°	0.1–0.4	33.02°

$$\dot{v} = (Y - \tfrac{1}{2}\rho L^2 d(m' + m'_x)ru)/(\tfrac{1}{2}\rho L^2 d(m' + m'_y))$$

$$\dot{r} = N/(\tfrac{1}{2}\rho L^4 d(I'_{zz} + J'_{zz})) \quad (7)$$

The above set of Eqs. (7) could be integrated once to obtain velocities, while displacement of motion is obtained with a single

Table 3
Comparison of hydrodynamic coefficients.

Symbol	Hydrodynamic coefficients value			
	Deep water ($h/d>3$)		Shallow water ($h/d=1.3$)	
	Empirical[1]	PMM	Empirical[1]	PMM
X'_{uu}	0.0162	0.0174	0.040	0.1875
$X'_{\beta r}$	0.0509	0.3124	0.0509	1.9588
Y'_{β}	0.2646	0.5967	1.2396	2.4193
Y'_{r}	0.0070	0.2501	−0.4351	−1.0408
$Y'_{\beta\beta}$	0.5269	0	1.8385	0
Y'_{rr}	−0.0141	0	0.0232	0
$Y'_{\beta\beta r}$	−0.1239	−1.7505	1.0400	4.4692
$Y'_{\beta rr}$	0.4934	2.0189	3.5500	2.6048
N'_{β}	0.0788	0.0383	0.4172	0.2081
N'_{r}	−0.0366	−0.0188	−0.1126	−0.0737
$N'_{\beta\beta}$	0.0140	0	0.0331	0
N'_{rr}	−0.0245	0	−0.0647	0
$N'_{\beta\beta r}$	−0.1750	−0.3262	−0.2193	−1.5483
$N'_{\beta rr}$	−0.0254	−0.1190	−0.0312	−0.5450
$Y'_{\beta\beta\beta}$	–	1.4556	–	6.2548
Y'_{rrr}	–	0.0387	–	2.4542
$N'_{\beta\beta\beta}$	–	−0.0049	–	0.0398
N'_{rrr}	–	0.0086	–	0.0578

integration to the velocities (Maimun et al., 2002):

$$u=\int \dot{u}\,dt \text{ and } x=\int u\,dt$$
$$v=\int \dot{v}\,dt \text{ and } y=\int v\,dt$$
$$r=\int \dot{r}\,dt \text{ and } \psi=\int r\,dt$$
$$\ddot{\psi}=\dot{r} \text{ and } \psi=\dot{r} \quad (8)$$

4.2. Simulation data

The simulation input data, which is a combination of hydrodynamic parameters and forces of hull, rudder and propeller, must firstly be determined before the pusher barge simulation of manoeuvring pusher barge can begin. The effect of hydrodynamic force, which incorporates the rudder, propeller and hull is included in the simulation together with equation of motion (Maimun et al., 2005).

Hydrodynamic force composes of three components namely the bare hull, propeller, and rudder force components, which are determined by their respective source (Yoon and Rhee, 2003). Tables 4 and 5 show the propeller diameter and rudder area used in the simulation. Prediction of resistance component was carried out in Universiti Teknologi Malaysia towing tank. The resistance and propulsion components are one of the parameters in the simulation programme. Rudders area is calculated based on Det norske Veritas (DnV) for minimum rudder area and the calculation of rudder area coefficient is referred to Crane et al. (1989). For vessel with increased manoeuvrability, rudder area coefficient are estimated 2–4 percent of $L\times d$ (Maimun et al., 2005).

5. Results

The simulation results illustrate a comparison of experimental and empirical results of ship motion in both deep and shallow water conditions. The result of ship motion is based on manoeuvring ability test such as turning circle test and zig-zag manoeuvre.

Table 4
Propeller and rudder parameters.

Item	Deep water	Shallow water-$h/T=1.3$
Ship speed, V (knots)	7	7
Number of propellers	2	2
P/D	0.74	0.74
Number of blades (Z)	4	4
Diameter, D (m)	2.67	2.67
Blade area ratio, EAR	0.461	0.461
Revolutions, RPS (n)	2.0636	2.7415
Wake fraction (w_{po})	0.299	0.4236
Trust deduction (t)	0.2	0.254
Advance ratio (J_p)	0.458	0.275
Thrust coefficient (K_T)	0.173	0.238
η_o	0.525	0.33
Thrust, T (kN)	76.825	193.29
C_0, C_1, C_2	0.3139; −0.2736; −0.1048	0.3139; −0.2736; −0.1048
Wake fraction (w_{Ro})	0.3189	0.4395
Rudder high (m)	2.5	2.5
Rudder area (m^2)	10.00 ($NP=2$)	10.00 ($NP=2$)
Number of rudders	2	2

Table 5
Turning circle parameters based on experimental data.

h/T	Indices	Experimental (m)	IMO standards	Correspond
Deep water	Advance	254	< 531 m or 4.5 L	Yes
	Tactical diameter	265	< 590 m or 5.0 L	Yes
1.3	Advance	360	< 531 m or 4.5 L	Yes
	Tactical diameter	410	< 590 m or 5.0 L	Yes

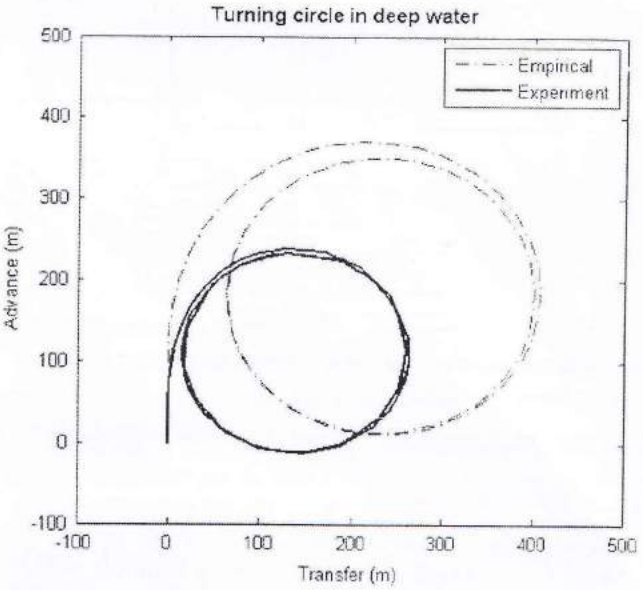

Fig. 10. Comparison of simulated turning trajectories in deep water condition between empirical and PMM test [$H/d=26.5$, where ship speed is 7 Knots].

5.1. Comparison of empirical and experimental results

The series of Figs. 10–12 display the empirical and experimental results obtained from the simulation programme in deep water condition. The advance and tactical diameter of experimental result in Fig. 10 are smaller as compared to the empirical result's diameter. Figs. 11 and 12 show a higher value of overshooting angle for empirical as compared to experimental result for 10/10 and 20/20 zig-zag manoeuvre.

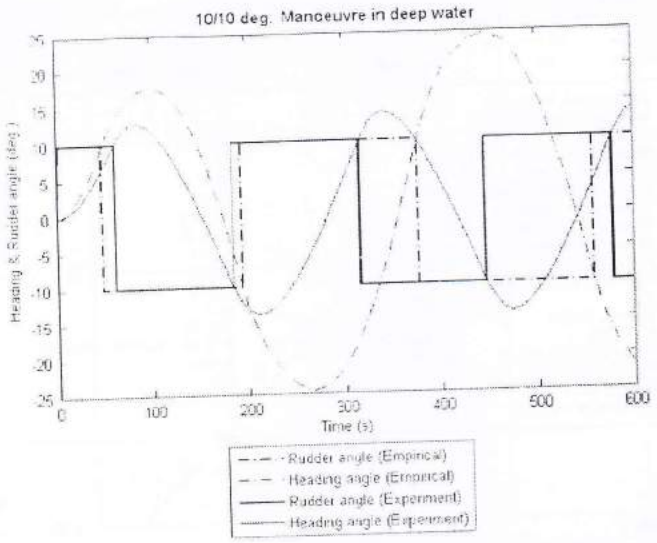

Fig. 11. Comparison of time histories of 10/10 zig-zag for deep water [speed = 7 Knots].

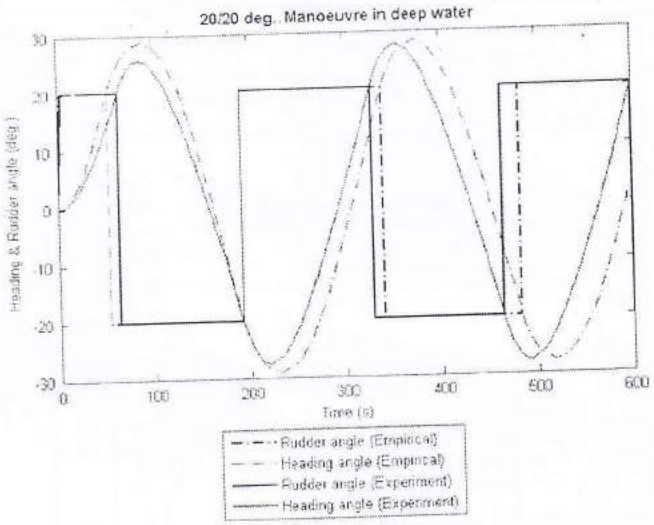

Fig. 12. Comparison of time histories of 20°/20 zig-zag [speed = 7 Knots].

5.2. Comparison of results for deep and shallow water conditions

5.2.1. Turning ability

The comparison of results in both deep and shallow water conditions are illustrated in Figs. 13–16. Figs. 13 and 14 show a smaller advance and tactical diameter for deep water condition. However, the empirical result shows a slower response of turning trajectory in deep water as compared to shallow water.

5.2.2. Zig-zag manoeuvre

The 10/10 zig-zag manoeuvre result in Fig. 15 demonstrates a larger overshoot angle in shallow water. However, the difference of overshoot angle between deep and shallow water is less obvious in Fig. 16 in the 20/20 zig-zag manoeuvre.

6. Discussion

The simulation results of the manoeuvring capability of the push barge are dependent on the input of hydrodynamic

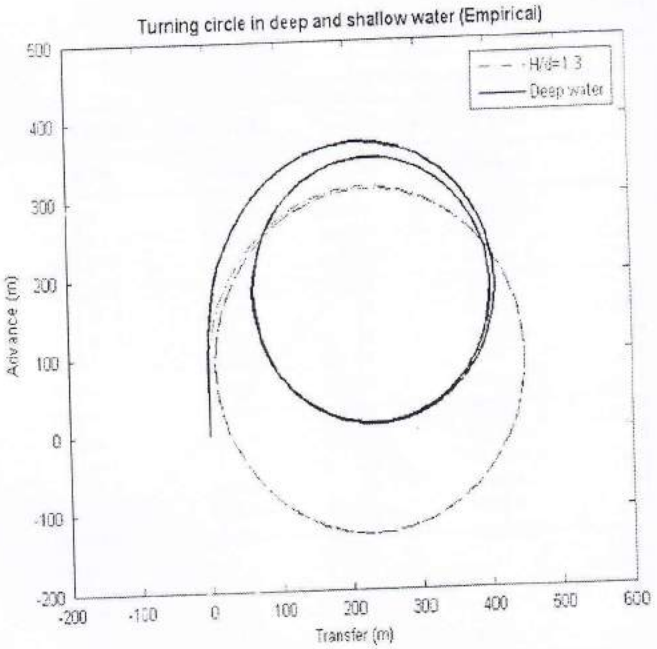

Fig. 13. Comparison of simulated turning trajectories in deep and shallow water based on empirical equations.

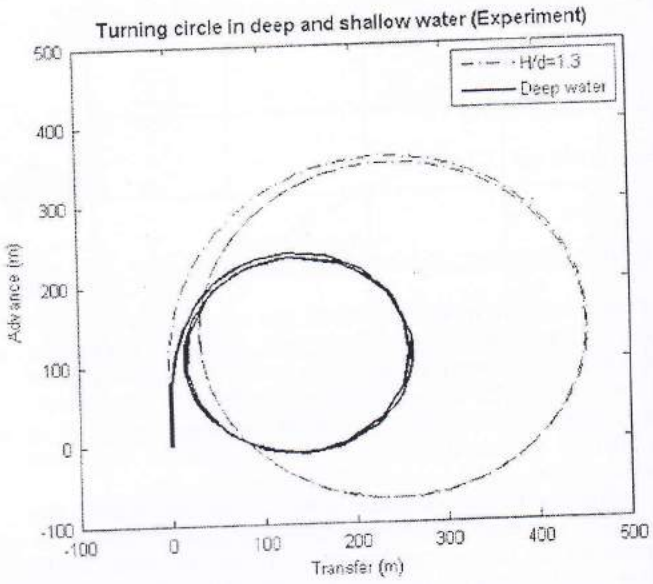

Fig.14. Comparison of simulated turning trajectories in deep and shallow water based on experimental results.

coefficients as well as the hull and rudder parameters. Thus the divergences of results in the experimental and empirical methods are mainly due to some error during the experiment or model preparation. Errors such as noise during data collection from the experiment are normally present. However, the result generated from the simulation on the turning circle and zig-zag manoeuvring test based on experimental method illustrate better manoeuvring properties as compared to empirical approach.

The turning circle results have satisfied the IMO standards by not exceeding the IMO advance and tactical diameter. However, the same could not be said to the zig-zag manoeuvre result as the overshoot angle for shallow waters exceeds the IMO standards. One of the main causes of for exceeding overshoot angle is design

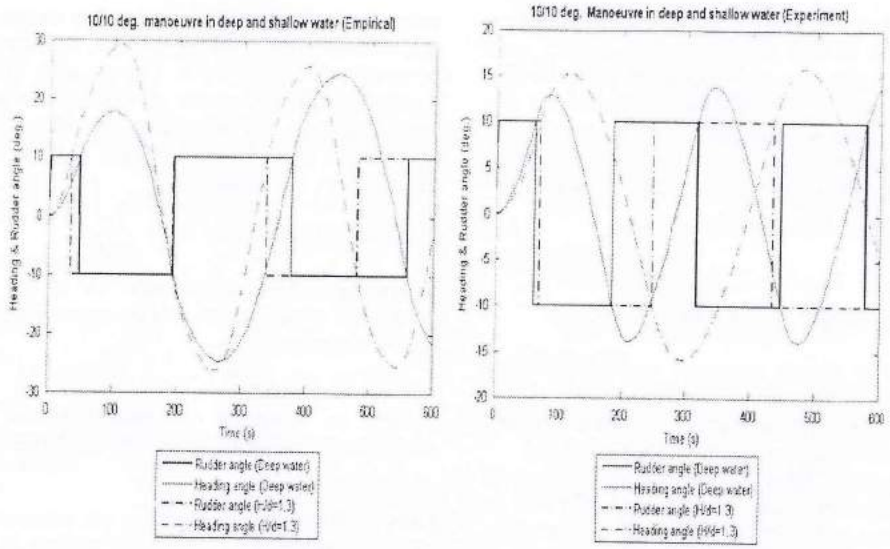

Fig. 15. Comparison of time histories of 10°/10° zig-zag for deep and shallow water ($H/d=1.3$) [speed=7 Knots].

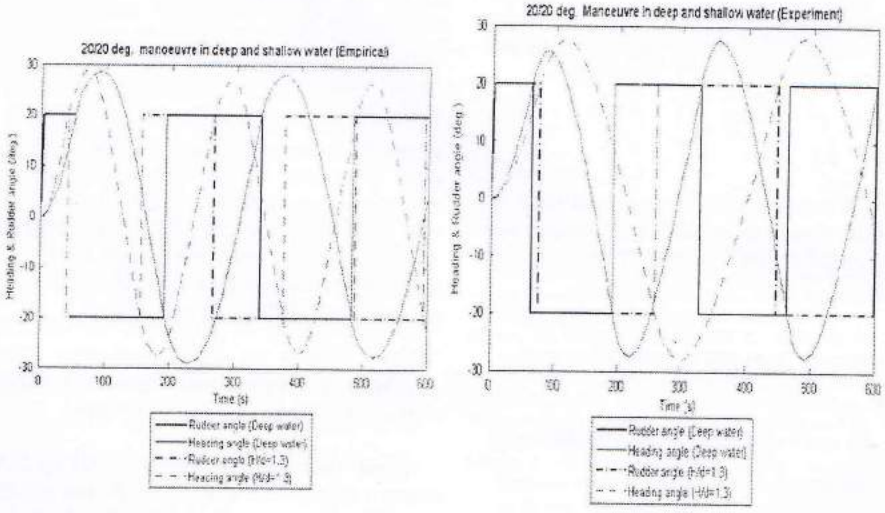

Fig. 16. Comparison of time histories of 20°/20° zig-zag [speed=7 Knots].

of the pusher-barge system. Thus, further studies on the hull design for the pusher-barge system might improve the zig-zag manoeuvre result.

The comparison of experimental and empirical results for turning circle shows that the experimental result has a better manoeuvring characteristic based on IMO standards. The zig-zag manoeuvre result shows that the empirical result has a higher overshoot angle as compared to the experimental result. A comparison of the 10°/10° zig-zag manoeuvre in Fig. 15 illustrates an irregular overshoot angle of the empirical result whereby the difference of the first and third overshoot is around 5°.

The comparison result of turning circle for both deep and shallow water conditions in Fig. 13 shows deep water condition has a tendency to have a smaller turning circle diameter as compared to the shallow water condition. A smaller turning circle indicates higher turning angle rate for a deep water condition. The turning circle results show that the deep water has a higher course changing capability as compared to shallow water condition. The relationship of the turning circle test in the context of push barge operation in confined and normally shallow waterways such as in canals and river inlet raises complication as the vessel needs a good course changing capability to avoid grounding effects and collisions.

Two standard time history of zig-zag manoeuvre result namely the 10°/10° and 20°/20° for both shallow and deep water conditions provide estimation on the vessel ability to enter into turning motion. Results for both rudder angles signify a higher overshoot of heading angle for shallow as compared to deep water condition. However an increase of rudder angle indicates a small difference of overshoot between the two conditions. The increment of rudder angle produces larger moment acting on the vessel, which counters the opposite yaw motion. However, vessel's response towards the change of rudder angle and moment depends on the flow field around the hull. Constraints of flow field around the hull in shallow water will reduce the rudder efficiency.

The combination of turning circle and zig-zag manoeuvre test suggests shallow water conditions have a significant impact on the manoeuvring characteristic of push barge. Operations of a push barge in shallow water are confined to several limitations such as difficulty in course changing capability as well as low rudder response. These limitations require a great deal of navigation experience as well as high dependency of navigation aid.

The result of the simulation can be further utilized in the future to analyze the correlation of ship manoeuvring capability with finite depth condition by adding more ratio of water depth to ship draught (H/d) condition. Since the simulation incorporated the rudder parameters, a recommended future research of analyzing the correlation of increment of rudder area to the manoeuvrability of pusher barge could be done with experimental validation

7. Conclusion

This research can be concluded as follows:

(a) The simulation result of zig-zag manoeuvr and turning circle shows that the experimental derived coefficient tend to give better manoeuvring characteristic as compared to the empirically derived coefficient based on agreement with IMO standards.
(b) The comparison of manoeuvring properties of deep and shallow water conditions show that a pusher barge has difficulty in manoeuvring in shallow water due to constrains such as complexity in course keeping and high overshoot heading angle.
(c) This research can be further developed by determining the correlation of finite water depth and rudder area with manoeuvrability of the pusher-barge by varying the water depth to ship draught ratio (H/d) as well as increasing rudder area of the pusher barge.

Acknowledgement

The authors would like to express their sincere gratitude to Prof. Chengi Kuo from the University of Strathclyde, Glasgow for his invaluable advice and comments given during the preparation of this paper.

Appendix A. Force and moment induced by propeller and rudder

X_P, Y_P, N_P and X_R, Y_R, N_R are expressed as the following formulas

$$X_P = C_{tp}(1-t_p)n^2D_p^4K_T(J_P)$$
$$Y_P = 0$$
$$N_P = 0$$
$$X'_P = \frac{X_P}{\frac{1}{2}\rho LdU^2}$$

where

$$K_T(J_P) = C_1 + C_2J_P + C_3J_P^2$$
$$J_P = U\cos\beta(1-w_P)/(nD_P)$$
$$w_P = w_{P0}\exp(-4.0\beta'^2_P)$$
$$\beta'_P = \beta - x'_P r'$$
$$x'_P \cong -0.5$$

where t_p is the thrust reduction coefficient in straight forward moving, C_{tp} the constant, n the propeller revolution, D_p the propeller diameter, w_p the effective wake fraction coefficient at propeller location, w_{p0} the effective wake fraction coefficient of propeller in straight running, K_T is the thrust coefficient of a propeller force, J_P the advance coefficient, and C_1, C_2, and C_3 are the constants for propeller open characteristics.

The terms and the non-dimensional of ruder forces describes as the following.

$$X_R = -(1-t_R)F_N\sin\delta$$
$$Y_R = -(1+a_H)F_N\cos\delta$$
$$N_R = -(x_R + a_Hx_H)F_N\cos\delta$$

where x_R is the the distance between the centre of gravity of shi and centre of lateral force ($x_R = x'_RL$) and x_R represents the locatio of rudder ($=-L/2$), x_H is the distance between the centre c gravity of ship and centre of lateral force ($x_H = x'_HL$), δ is rudde angle, and t_P, t_R, a_H, and x_H are the interactive force coefficient among hull, propeller and rudder. F'_N is rudder normal force an described as the following:

$$F'_N = (A_R/Ld)C_NU_R^2\sin\alpha_R, \quad F'_N = \frac{F_N}{\frac{1}{2}\rho Ld}$$

where A_R is the rudder area, C_N is the gradient of the lif coefficient of ruder, and can be approximated as the function o rudder aspect ratio K_R.

$$C_N = 6.13K_R/(K_R+2.25)$$

U_R and α_R represent the rudder inflow velocity and angle respectively; they can be described as the following.

$$U_R^2 = (1-w_R)^2\{1+Cg(s)\}$$
$$g(s) = \eta K\{2-(2-K)s\}s/(1-s)^2$$
$$\eta = D_P/h_R$$
$$K = 0.6(1-w_p)/(1-w_R)$$
$$s = 1.0-(1-w_p)U\cos\beta/nP$$
$$w_R = w_{RO}w_P/w_{PO}$$
$$\alpha_R = \delta - \gamma\beta'_R$$
$$\beta'_R = \beta - 2x'_Rr'$$
$$x'_R \approx -0.5$$

where A_R is the rudder area, h_R the rudder height, K_R the aspect ratio of rudder, U_R the effective rudder inflow speed, α_R the effective rudder inflow angle, C the coefficient for starboard and port rudder, w_R the effective wake fraction coefficient at rudder location, w_{RO} the effective wake fraction coefficient at rudder location in straight forward motion, P the propeller pitch, and γ the flow straightening coefficient.

Appendix B. Approximate formulae of hydrodynamic coefficients in deep water by Kijima

These formulae are function of ship length (L), breadth (B), draught (d), block coefficient (CB) and aspect ratio of ship hull k; ($k=2d/L$). However, the prediction formulas proposed by Mori (1995) are for four parameters, which are e_a, e'_a, σ_a and K to express the characteristics of aft hull shape. The coefficients e_a and e'_a express fullness of aft run and σ_a is aft sections fullness metric, while K is the form factor. The parameters are defined by principal particulars with water plane area coefficient C_{wp} and prismatic coefficient C_{pa} of aft hull between A.P.:

$$e_a = \frac{L}{B}(1-C_{pa})$$
$$e'_a = e_a\Big/\sqrt{\frac{1}{4}+\frac{1}{(B+d)^2}}$$
$$\sigma_a = \frac{1-C_{wp}}{1-C_{pa}}$$
$$K = \left(\frac{1}{e'_a}+\frac{1.5}{L/B}-0.33\right)(0.95\sigma_a+0.40)$$

The engagement of these parameters together with a model database of 15 kinds of ships and 48 loading conditions generates a series of approximate of hydrodynamic coefficients as follows:

$$Y'_\beta = 0.5\pi kk + 1.9257\left(\frac{CB}{L}\right)\sigma'_a$$
$$Y'_\beta - (m'+m'_x) = 0.25\pi k + 0.052e'_a - 0.457$$
$$Y'_{\beta\beta} = -1.199CB\sigma_a + 1.05$$

$$Y'_{\beta} = 0.225\left(\frac{dCB}{B}\right)e'_a - 0.12$$

$$Y'_{\beta rr} = 7.1256\left\{\frac{d(1-CB)}{B}\right\}$$

$$Y'_{\beta\beta r} = 10.443\left[\left\{\frac{d(1-CB)}{B}\right\}e'_a\right]^2 - 9.374\left\{\frac{d(1-CB)}{B}\right\}e'_a + 1.227$$

$$N'_{\beta} = k\left[150.668\left\{\left\{\frac{d(1-CB)}{B}\right\}e'_aK\right\}^2 - 23.819\left\{\frac{d(1-CB)}{B}\right\}e'_aK + 1.802\right]$$

$$N'_r = -0.54k - k^2 - 0.0477e'_aK + 0.0368$$

$$N'_{\beta\beta} = 0.15K - 0.068$$

$$N'_{\beta rr} = -0.4086CB + 0.27$$

$$N'_{\beta\beta r} = -0.826\left\{\frac{d(1-CB)}{B}\right\}e' - 0.026$$

Appendix C. Approximate formulae of hydrodynamic coefficients in shallow water

The approximate formulae for estimating the hydrodynamic force acting on a ship in shallow water was proposed by (Kijima et al., 1990). These formulas are obtained semi-empirically from the results of numerical calculations based on lifting surface theory, and model tests in full load condition. The formulae for full load condition can be applied to the case of shallow water by correcting the hydrodynamic coefficients and coefficients, which have been originally obtained for deep water (Maimun et al., 2005).

Estimation of the hydrodynamic force acting on a ship in shallow water can be done as follows:

$$D_{shw} = f(h)XD_{dep}$$

where D_{shw} is the coefficients in shallow water including ballast and half load conditions, D_{dep} the coefficients in deep water, including ballast and half load conditions, and $f(h)$ the correcting factor, $h=d/H$ (d is draught, H is water depth).

The correcting factor $f(h)$ for the effect of water depth is divided into two different equations, which are applied based on a certain hydrodynamic coefficients. The correcting factors $f(h)$ are as followed:

(a) Correcting factor, $f(h)$ for hydrodynamic coefficients Y'_{β}, $Y'_{\beta\beta}$, $Y'_{\beta rr}$, N'_{β} and N'_r:

$$f(h) = [1/(1-h)^n] - h$$

where, for instance, Y'_{β}, $n=0.4CB$ (B/d); $Y'_{\beta\beta}$, $n=-0.26CB$ $(B/d)+1.74$; $Y'_{\beta rr}$, $n=-2.13CB/B+1.8$ (5.7); N'_{β}, $n=0.425 \times CB \times B/d$; N'_r, $n=-7.14k+1.5$

(b) Correcting factor $f(h)$ for other hydrodynamic coefficients:

$$f(h) = 1 + a_1h + a_2h^2 + a_3h^3$$

where for instance,

(i) For, $Y'_{\beta} - (m' + m'_x)$:
$a_1 = -5.5(CB(B/d))^2 + 26CB(B/d) - 31.5$
$a_2 = 37(CB(B/d))^2 - 185CB(B/d) + 230$
$a_3 = -38(CB(B/d))^2 + 197CB(B/d) - 250$

(ii) For, Y'_{rr}:
$a_1 = -0.15 \times 105(1-CB)^5$
$a_2 = 1.16 \times 105(1-CB)^5$
$a_3 = -1.28 \times 105(1-CB)^5$

(iii) For, $Y'_{\beta\beta r}$:
$a_1 = 2.15 \times 10^4((d(1-CB)/B)^2) - 0.48 \times 10^4 d(1-CB)/B + 220$
$a_2 = -4.08 \times 10^4((d(1-CB)/B)^2) - 0.75 \times 10^4 d(1-CB)/B - 274$
$a_3 = -9.08 \times 10^4((d(1-CB)/B)^2) + 2.55 \times 10^4 d(1-CB)/B - 1400$

(iv) For, $N'_{\beta\beta}$:
$a_1 = -0.24 \times 10^3(1-CB) + 57$
$a_2 = 1.77 \times 10^3(1-CB) - 413$
$a_3 = -1.98 \times 10^5(1-CB) + 467$

(v) For, N'_{rr}:
$a_1 = -0.196 \times 10^4((d(1-CB)/B)^2) + 448d(1-CB)/B - 25$
$a_2 = 1.222 \times 10^4((d(1-CB)/B)^2) - 2720d(1-CB)/B + 446$
$a_3 = -1.216 \times 104((d(1-CB)/B)^2) + 2650d(1-CB)/B - 137$

(vi) For, $N'_{\beta\beta r}$:
$a_1 = 0.91 \times 10^2 CB(d/B) - 25$
$a_2 = -5.15 \times 10^2 CB(d/B) + 144$
$a_3 = 5.08 \times 10^2 CB(d/B) - 143$

(vii) For, $N'_{\beta rr}$:
$a_1 = 0.4 \times 10^3 CB(B/d) - 88$
$a_2 = -2.95 \times 10^3 CB(B/d) + 645$
$a_3 = 3.12 \times 10^3 CB(B/d) - 678.$

References

Beukelman, W., Journee, J.M.J., 2001. Hydrodynamic transverse loads on ships in deep and shallow water, HADMAR'2001, in: Proceedings of the 22nd International Conference on Hydrodynamics and Aerodynamics I, Marine Engineering.

Crane, C.L., Eda, H., Landsburg, A., 1989. Controllability Chapter IX. Principle of Naval Architecture Second Revision Vol. III.

Kijima., K., Nakiri, Y., Furukawa, Y., 2000. On the Prediction Method for Ship Manoeuvrability, in: Proceedings of International Workshop on Ship Manoeuvrability, Hamburg Ship Model Basin, Germany, Paper No. 7.

Kijima, K., Nakiri, Y., Tsusui, Y., Matsunaga, M., 1990. Prediction method of ship manoeuvrability in deep and shallow waters. MARSIM and ICSM, vol. 90, Tokyo, Japan.

Lataire, E., Vantorre, M., Laforce, E., Eloot, K., Delefortrie, G., 2007. Navigation in Confined Waters: Influence of Bank Characteristics on Ship-Bank Interaction, in: Proceedings of Second International Conference on Marine Research and Transportation, June 2007, Ischia, Itali.

Maimun, A., Atef, S., Muhammad, A.H., 2005. Manoeuvring of Pusher-Barge in Deep and Shallow Water, in: Proceedings of Tenth JSPS Marine Transportation Engineering Seminar, Hiroshima, Japan.

Maimun, A., Loh, S.P., Lee, R., 2002. Manoeuvring Assessment of Fishing Vessel, in: Proceedings of 7th JSPS Marine Transportation Engineering Seminar, Hiroshima, Japan.

Mori, M., 1995. A note on hull form design (part 24). Journal of Ship Science 48, 40–49 (In Japan).

Vantorre,M., Eloot,K., 1996. Hydrodynamic Phenomena Affecting Manoeuvres at Low Speed in Shallow Navigation Areas, in: Proceedings of 11th International Harbour Congres, Antwerpen, Belgium, pp. 535–546.

Wang, D.J., Bakountouzis, L., Katory, M., 2000. Prediction of ship hydrodynamic derivatives in shallow water and restricted waters. International Shipbuilding Progress 47 (452), 379–396.

Yoon, H.K., Rhee, P.R., 2003. Identification of hydrodynamic coefficients in ship manoeuvring equations of motion by estimation-before-modeling technique. Ocean Engineering.